Nuclear Instruments and Methods in Physics Research A274 (1989) 217–221
North-Holland, Amsterdam

THE NEUTRON DETECTION EFFICIENCY OF NE213 DETECTORS MEASURED BY MEANS OF A ^{252}Cf SOURCE

J. CUB, E. FINCKH, K. GEBHARDT, K. GEISSDÖRFER, R. LIN and J. STRATE

Physikalisches Insitut, Universität Erlangen-Nürnberg, Erwin Rommel Str. 1, D-8520 Erlangen, FRG

H. KLEIN

Physikalisch-Technische Bundesanstalt, D-3300 Braunschweig, FRG

Received 27 June 1988

The neutron detection efficiency of a NE213 scintillator was determined by comparing the measured neutron time-of-flight spectrum of a ^{252}Cf source with its reference neutron energy distribution. Below $E_n = 8$ MeV an accuracy of better than 3% could be achieved. The measured efficiency agreed reasonably well in shape with a Monte Carlo simulation in the entire energy range 0.8 MeV $\leqslant E_n \leqslant$ 13 MeV, but the calculation is generally about 5% lower than the experimental values.

1. Introduction

Neutron flux measurements require the efficiency of the neutron detector to be known well. The neutron detection efficiency of NE213 liquid scintillation detectors, which are often used in time-of-flight (TOF) spectrometers due to their timing and n/γ discrimination properties, depends on the neutron energy, the actual threshold, the size of the scintillator (multiple scattering) and the mechanical setup of the detector system (inscattering). In principle, all these influences can be taken into account in Monte Carlo simulations of the detector response [1]. Even if recently evaluated cross section data [2] and individual light output and resolution functions are used, the accuracy of the calculations is chiefly limited by the uncertainties of these basic input data. Particularly the neutron-induced reactions on carbon become important for neutron energies above 7 MeV and for thresholds below about 2 MeV recoil proton energy.

For this reason, experimental tests are necessary. Various techniques are applied [3,4] which in general require an accelerator for neutron production and sophisticated methods to determine the neutron flux. With the exception of the ^{252}Cf neutron source, no other neutron source is available which has a well-defined energy distribution and allows the TOF technique to be applied [5]. Following the spontaneous fission, which can easily be detected, neutrons with a continuous energy spectrum are emitted. The energy distribution has been carefully investigated experimentally [6] and theoretically [7] and the evaluated shape [8] can be regarded as a reference. Ionization chambers with a thin Cf source on the inner electrode have been developed which are fast enough to process a fission rate larger than 10^5 s^{-1}, well separated from the α-decay rate which is about 30 times larger. Low mass ($\leqslant$ 3 g) and high fission-fragment detection efficiency (> 99%) guarantee that the primary neutron energy distribution is only slightly distorted [9].

2. Experimental setup

The experimental setup is schematically shown in fig. 1 and the most important parameters are summarized in table 1. Both the low-mass fission-fragment ionization chamber and the scintillation detector were mounted about 2.5 m above the floor in a large experimental hall in order to reduce the fraction of wall-scattered neutrons. A rest of this background and air inscattering could not be avoided and were measured by inserting a shadow bar exactly matching the size of both detectors and long enough to attenuate neutrons up to 10 MeV by a factor larger than 600 (25 cm iron, 45 cm paraffine).

The Cf chamber was constructed and carefully investigated at the Physikalisch-Technische Bundesanstalt. At the time of these investigations, a fission rate of 0.86×10^5 s^{-1} was measured with 99.5% efficiency.

The detector system to be investigated was assembled at the University of Erlangen. The glass-encapsulated liquid scintillator was directly coupled to a phototube in order to optimize the n/γ discrimination at a low threshold. The detector and the shadow bar were

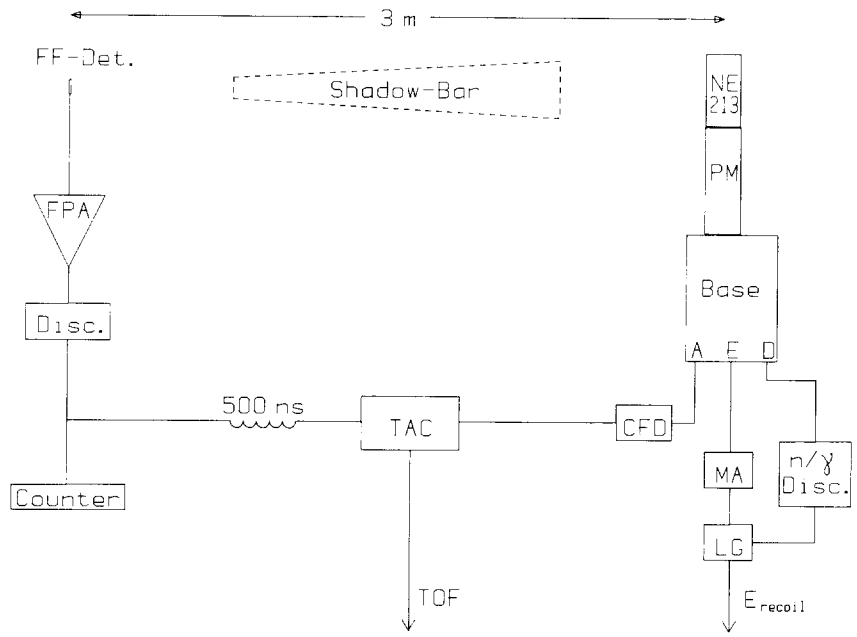

Fig. 1. Block diagram of the electronics. FF-Det.: fission fragment detector including ^{252}Cf source; FPA: fast preamplifier; Disc.: fast discriminator; NE213: liquid scintillator; PM: photomultiplier; A: anode output; E: integrated pulse height; D: dynode output; MA: main amplifier; n/γ Disc.: pulse shape analyzer; LG: linear gate; TAC: time-to-amplitude converter.

carefully aligned by means of a laser. As usual, the TOF measurements were performed in an inversed time scale.

Neutron- and gamma-induced events are separated by applying pulse shape analysis [10]. The pulse height taken from the 11th dynode and time-of-flight were stored in a two-dimensional list mode. In this way, TOF spectra could be generated for various thresholds and the pulse-height-dependent time walk could be corrected according to the behaviour of the prompt gamma peak (see section 4). Gain shifts were controlled by feeding LED signals into the scintillator.

Table 1
Properties of the ^{252}Cf source and the neutron detector

Cf source	
Cf mass	0.2 μg
Backing	0.2 mm Pt
Fission rate (during measurement)	86000 s^{-1}
Fission-fragment detection efficiency	(99.5 ± 0.2)%
Ionization chamber mass	≤ 3 g (Pt, Fe)
Deadtime (incl. discriminator)	530 ± 20 ns
NE213 detector	
Diameter	53 mm
Height	101 mm
Wall thickness of the glass vessel	1.5 mm
(Incoming neutrons perpendicular to the cylinder axis)	
Measurement conditions	
Flight path	3 m
TAC range	500 ns
TAC calibration factor	0.24 ns/channel
Recording time, open geometry	210 h
with shadow bar	120 h

3. The expected neutron TOF distribution

On the energy scale, the neutron energy density distribution $n(t)$ is described by a Maxwellian distribution, slightly modified by a correction function. The

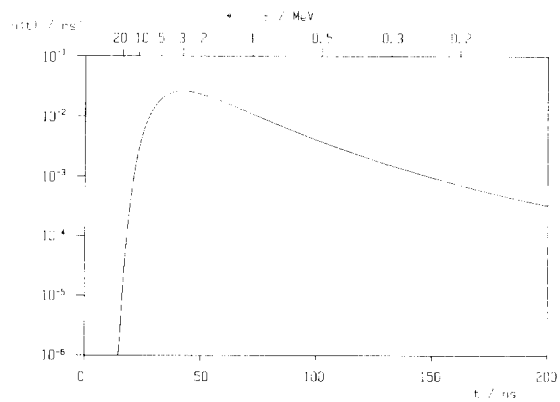

Fig. 2. Reference density distribution $n(t)$ of the neutrons from a ^{252}Cf neutron source versus flight time for a 1 m flight path.

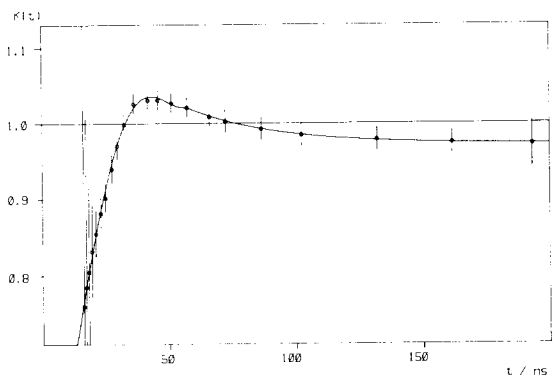

Fig. 3. Correction function $K(t)$ which gives the deviation of the evaluated ^{252}Cf spectrum from a Maxwellian distribution. The data points and error bars are taken from ref. [8]; the line shows the polynomial fit given in the text.

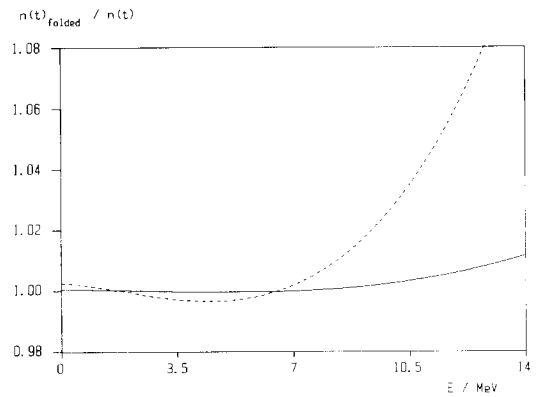

Fig. 5. Effect of the finite time resolution on the Cf neutron spectrum. Full line: 3 m flight path, dashed line: 1 m.

Maxwellian distribution can easily be transferred onto the time scale if relativistic kinematics is used in first approximation [11] and yields (see fig. 2):

$$n(t) = \sqrt{\frac{b^3}{\pi}}\,\frac{4}{t^4}\left(1+\frac{5a}{2t^2}\right)\exp\left[-\frac{b}{t^2}\left(1+\frac{a}{t^2}\right)\right]K(t),$$

where $a = 8.345$ ns^2 is the relativistic correction parameter, $b = 3681.04$ ns^2 is the "temperature" parameter and t is the time of flight for a 1 m flight path.

The correction function was fitted for two time intervals (fig. 3):

$$K(t) = 0.49078 + 0.0099946t + 0.0008073t^2 - 2.6375\times10^{-5}t^3 + 2.1063\times10^{-7}t^4$$

for $t \leqslant 56.8$ ns;

$$K(t) = 0.973 + 0.2563\exp(-0.02902t)$$

for $t > 56.8$ ns.

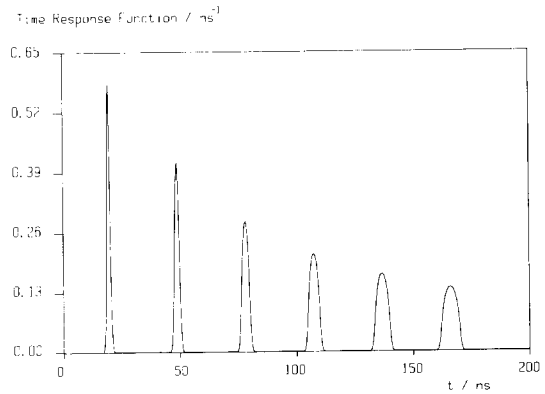

Fig. 4. Time response functions for six neutron energies (flight path 1 m). The line width is chiefly determined by the electronic time resolution for high neutron energies and by the flight time through the scintillator for low energies.

Next, the time response originating from the electronic time resolution and the size of the scintillator must be considered. The second contribution is an elliptical (rectangular) distribution for neutrons entering the scintillator perpendicular (parallel) to the cylinder axis. The electronic time jitter was determined by the prompt γ-peak and approximated by a Gaussian distribution (FWHM = (1.25 $\pm$ 0.05) ns). Fig. 4 shows examples of the time response calculated with these input data. The neutron flux attenuation in the detector was not taken into account, but its effect on a measured spectrum may be compensated by multiple-scattering effects.

Folding $n(t)$ with this time response produces the expected TOF neutron distribution $n_f(t)$. The correction is significant for short flight paths ($\sim$ 1 m) but almost negligible for distances longer than 3 m (see fig. 5). The properly folded time density distribution must be multiplied with the well-known neutron multiplicity $\bar{\nu} = 3.77$ [12], the solid angle and the total number of fissions counted during the measuring time, and corrected for dead-time losses and air attenuation. This calculated TOF spectrum is then compared with the experimental spectrum. It should be noted that the distortions due to the structural material of the fission chamber are small as long as only neutron energies above 1 MeV are measured.

4. The experimental TOF spectrum

With a 3 m flight path, the TOF spectra in open geometry (fig. 6) and with inserted shadow bar (fig. 7) were taken for 210 h and 120 h, respectively. Some of the nondiscriminated prompt gamma events indicate the time reference. The time reference was determined without n/γ discrimination and showed a significant

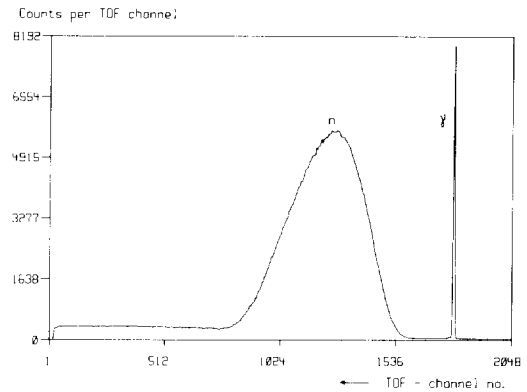

Fig. 6. Measured TOF neutron spectrum of the ^{252}Cf source (channel width 0.24 ns, flight path 3 m)

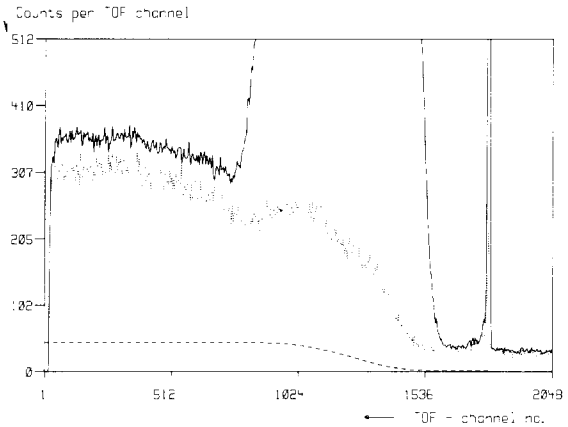

Fig. 7. Background TOF spectrum measured with shadow bar (dotted line), calculated background spectrum of uncorrelated stop-events (dashed line) and spectrum as in fig. 6 (solid line).

time walk (~ 1 ns overall) depending on the pulse height (fig. 8). All data were corrected for this effect.

Most of the background below the neutron threshold (around channel 800) is determined by the "shadow

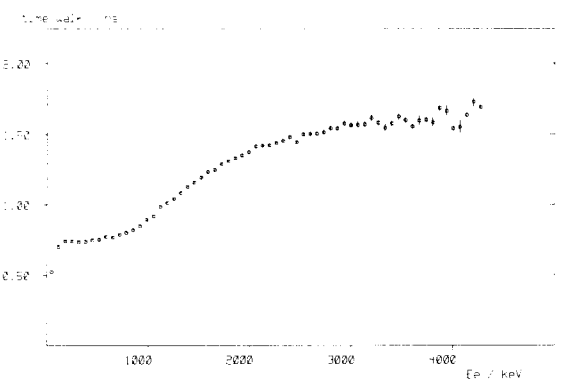

Fig. 8. Variation of time reference versus pulse height (time walk). Mean FWHM of the γ-line amounts to (1.25 ± 0.05) ns.

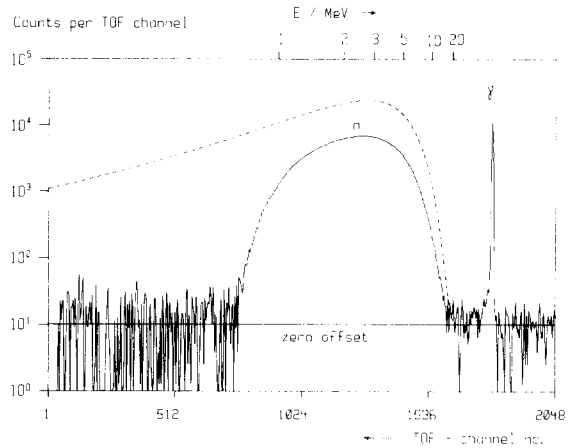

Fig. 9. Measured neutron TOF spectrum after background subtraction (solid line) and predicted TOF spectrum of a ^{252}Cf source (dashed line).

bar" run. The remaining fraction (fig. 7) originates from stop signals in the TAC not correlated with the detected neutron and must be calculated iteratively [9]. The final TOF spectrum (fig. 9) is divided by the expected distribution in order to extract the neutron detection efficiency for any particular threshold applied in the off-line analysis.

5. Discussion of the results

The experimental efficiency was transferred to the energy scale for a threshold equivalent to 150 keV electron energy (fig. 10). The energy intervals are non-equidistant and increase with the neutron energy. A list of the statistical and estimated systematic errors is given in table 2. In summary, we conclude that below 8 MeV neutron energy an uncertainty of 3% (1 standard devia-

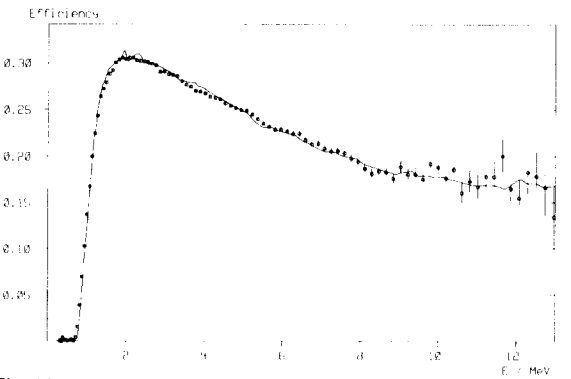

Fig. 10. Evaluated neutron efficiency for a NE213 detector and Monte Carlo simulation multiplied by 1.05 (solid line). The error bars contain statistical uncertainties only.

Table 2
Influence on the effiency ($\Delta\epsilon/\epsilon$) [%] of the various uncertainties

Flight path	3 m			1 m		
Neutron energy [MeV]	1	3	10	1	3	10
Time reference $\Delta t = 0.1$ ns	0.12	0.02	1.47	0.36	0.05	4.40
Time calibration $\Delta t/t = 1‰$	0.26	0.02	1.01	0.26	0.02	1.01
Flight path $\Delta s = 2$ mm	0.03	0.21	0.87			
$\Delta s = 1$ mm				0.04	0.32	1.30
Threshold $\Delta E_e = \pm 5$ keV	11	0.6	0.7	11	0.6	0.7
Statistical uncertainties (energy interval $\Delta E = 0.02E$) total recording time 330 h	0.84	0.46	4.38			
80 h				0.52	0.35	2.95

tion) is to be expected, chiefly limited by systematic errors, e.g. the uncertainty in the shape of the reference Cf neutron energy spectrum (~ 2%). Due to the exponential decrease in the neutron spectrum, the statistical uncertainties rapidly increase for higher energies.

Finally, we compared the measured efficiency with a Monte Carlo simulation, carried out with the latest version of the NRESP code [1]. Since the individual light output function had not been investigated, the calculation was performed with a trial function used at PTB for reference. In consequence, the effective threshold energy could not be taken from a Compton electron calibration but was chosen to fit the behaviour of the experimental efficiency near the threshold (fig. 10). In fact, the shape is very well reproduced for the entire energy region but the calculated efficiency must be increased by about 5%. With respect to the restrictions of the calculation and the uncertainties estimated, the agreement seems to be satisfactory, pariticularly if we consider that the assumed volume and chemical composition of the detector may be uncertain.

6. Conclusion

Calibration of neutron detectors with a ^{252}Cf source is a relatively easy and practical method which gives good results for neutron energies below 10 MeV. It should be noted, however, that the use of short flight paths (~ 1 m) is unreliable. The main advantage of a short distance is the higher neutron flux. Furthermore the relative fraction of background (wall scattering, air inscattering and uncorrelated stops) decreases with the flight path. On the other hand, the influence of the finite time resolution is a decisive disadvantage. A correct consideration of the time response resulting from the effects of electronical time jitter and the size of the scintillator (including flux attenuation and multiple scattering) requires detailed investigations theoretically and experimentally and can therefore not be performed to date. For longer flight paths ($\geq$ 3 m), this correction is not important and the accuracy in TOF measurements (see table 2) is much better. Nevertheless, relative calibrations can be done with shorter flight paths, e.g. to check the equality of a set of detectors.

Acknowledgements

The authors wish to thank Dr. R. Böttger for preparing and specifying the Cf source. The Erlangen group gratefully acknowledges financial support of the Deutsche Forschungsgemeinschaft.

References

[1] G. Dietze and H. Klein, PTB-report ND-22, Braunschweig (1982).
[2] Evaluated Nuclear Data File ENDF/B-V, Brookhaven (1979).
[3] M. Drosg, Nucl. Instr. and Meth. 105 (1972) 573.
[4] J.L. Fowler, J.A. Cookson, M. Hussain, R.B. Schwartz, M.T. Swinhoe, C. Wise and C.A. Uttley, Nucl. Instr. and Meth. 175 (1980) 449.
[5] A. Smith, P. Günther and R. Sjoblom, Nucl. Instr. and Meth. 140 (1977) 397.
[6] W. Boldeman (review), IAEA-TECDOC-410 (1987) 125.
[7] H. Märten (review), IAEA-TECDOC-410 (1987) 144.
[8] W. Mannhart, IAEA-TECDOC-410 (1987) 158–170
[9] R. Böttger, H. Klein, A. Chalupka and B. Strohmaier, Proc. Int. Conf. on Nuclear Data for Science and Technology, ed. K.H. Böckhoff (Reidel, Dordrecht, 1983) p. 484.
[10] H. Blank et al., Nucl. Instr. and Meth. A240 (1985) 311.
[11] J. Cub, Diplomarbeit, Erlangen (1987) unpublished.
[12] R.R. Spencer, special publication, NBS-544 (1980) 728.